Analysis of the Dynamic Behavior of the Ventilation Duct, for a Varied Range of Air Flow and Wall Thicknesses for the Long Circular Duct

Dan ION*
Institute of Solid Mechanics of the Romanian Academy, 15 Constantin Mille Str., 010141 Bucharest, Romania, dan.ion@imsar.com, dan.ion@icecon.ro

Andrei-Cristian COTOBAN
Institute of Solid Mechanics of the Romanian Academy, 15 Constantin Mille Str., 010141 Bucharest, Romania, andrei.cotoban@imsar.ro

Polidor BRATU
Institute of Solid Mechanics of the Romanian Academy, 15 Constantin Mille Str., 010141 Bucharest, Romania, icecon@icecon.ro

* Author to whom correspondence should be addressed

Abstract: - The present paper approaches the analysis of the dynamic behavior induced by different values of air flow, which correspond with specific speeds of air, for the circular ventilation ducts, for a varied range of air flow rates and of wall thicknesses of the air passage channels. The study focuses on airflow-induced vibrations and the possibility of resonance in certain sections of the ventilation system [2], as well as the causes and effects of turbulent airflow in ventilation systems, which can negatively impact pipes and their supports. Using the Bentley AutoPIPE CONNECT Advanced Edition software for the ventilation air ducts, we perform a modal analysis and simulate the displacements on the three axes, the forces and moments additionally induced on the piping system, factors that contribute significantly to the weight of the system of air ducts, with another amplificant factors depending on pressure and temperature. Based on seven different air flow values and corresponding specific air speed values in the duct system, the specific turbulent regimes were calculated, and the different excitation frequencies were obtained. That excitation frequency is compared with the frequency corresponding to the maximum mass influence, obtained on the modal analysis, with the final scope being to completely evaluate these effects of the Vortex-Induced Vibration (VIV) mechanism [3] associated with the periodic appearance of vortices in areas with geometric discontinuities, respectively, in the vicinity of bends. The characterization of the phenomenon was achieved using the Reynolds and Strouhal numbers, which describe the oscillatory nature of the airflow and allow the estimation of the vortex shedding frequency.
The final scope is as follows: in the first part, determining the value of the most unfavorable frequency obtained through modal analysis with the Bentley AutoPIPE CONNECT Advanced Edition software; and in the second part, calculating the excitation frequency from air turbulence. Thus, obtaining the most unfavorable value of the frequency, a technical parameter that leads to the destruction of the air ducts, results in the loss of airtightness as well as the destruction of the air transport installation.

Keywords: - modal analysis, air flow in tubular ducts, eigenmodes, harmonic disturbing forces, vibrations.

1. INTRODUCTION

The study focuses on the vibrations induced by airflow through ventilation duct systems [1] with lengths greater than 30 m, as well as on the possibility of resonance [2] occurring in certain sections of the ventilation system.

Analyzing the dynamic behavior of a long circular ventilation duct with varied airflow and wall thicknesses involves using Computational Fluid Dynamics (CFD), focusing on pressure losses, turbulence, and structural responses (vibrations/stress) to understand efficiency and potential issues like noise or fatigue, often compared with experimental data from tests for validation, optimizing design for energy efficiency and comfort.

Key factors include Reynolds number, turbulence models, wall material properties (thickness, stiffness), and transient flow conditions, leading to conclusions on airflow distribution, pressure drop, and structural integrity.

To evaluate these factors and effects, the Vortex-Induced Vibration (VIV) mechanism [3], [28] was considered associated with the periodic detachment of vortices in areas with geometric discontinuities, respectively, in the vicinity of bends.

Until the present, other researchers made studies from the point of view of flow-induced vibration in pipes [3], or from the point of view of the influence of the tee connection with the pipe [28]. We perform a study of the long duct that includes the straight ducts that are connected by the four elbows, with a cumulative length of the entire aero-transport system of 30 meters.

The novelty consists in the fact that for a certain section, the real ducts are equipped with the support and embedment systems that were made based on a project carried out 35 years ago, using the Bentley AutoPIPE CONNECT Advanced Edition software.

We perform simulated with the Bentley AutoPIPE CONNECT Advanced Edition software and we obtaind the values of specific parameters of air flow, spedd, and other specific parameters, performing the change in the thickness of the air channel, respectively from 2 mm as the thickness is, we simulated with the software thicknesses of 4 mm or 6 mm.

We also simulated different air flows (from 1000 m^3/h to 7000 m^3/h) with the final goal of monitoring parameters that negatively influence the functionality (sealing) of the air transport system. Thus, it was highlighted that for the three thicknesses of the air duct, a dangerous frequency, a resonance frequency, with the approach value of 15Hz is obtained, which corresponds to an air flow rate of 4000 mc/h, a flow rate that is also commonly used under normal operating conditions.

The synthesis of the work is based on a modal analysis with the software Bentley AutoPIPE CONNECT Advanced Edition, through a modal analysis on which we superimposed one sinthess based on the flow rate variation determining the most unfavorable, respectively the most destructive resonance frequency which will have as a final effect the loss of tightness at the joints of the air transport pipe, in the area of the elbows.

The problem of vibrations in pipeline systems [4] must be carefully analyzed and monitored because it leads to the fatigue of the material from which the pipes are made, with consequences on the process of air transport, which they are part of.

The consequences, such as breaking and cracking in the welded area, are significant and must be avoided.

Dangerous movements are the axial movements of the component parts of the ventilation-air conditioning network, principally for ducts, in the direction of air circulation from the source to the user, which lead to the loss of the tightness of the parts from the designed parameters.

The HVAC systems use different technologies, with the scope to control the inlet or outlet of air parameters of temperature, humidity, and air purity in a closed space as follows: H represents the abbreviation for heating systems, V represents the abbreviation for ventilation systems, and AC represents the abbreviation for air conditioning systems.

2. TECHNICAL FACTORS AND CAUSES THAT CONDUCT THE APPEARANCE OF VIBRATIONS

There are 5 main principal causes of the occurrence of critical vibrations in pipeline systems longer than 30 m, with specific technical solutions [4], as follows:

a. Unbalanced components

One of the most frequent causes of excessive HVAC vibration stems from unbalanced rotating components. Fans, motors, and blowers, which are integral to air movement within HVAC systems, can become unbalanced over time due to dirt buildup, uneven wear, or slight manufacturing imperfections [5], [6].

An unbalanced rotor generates centrifugal forces that manifest as destructive vibrations, accelerating bearing wear, overheating motor windings, and increasing operational noise of intire air HVAC system [7].

The technical solution: Regular cleaning of fan blades, dynamic balancing by trained technicians, and the use of **Spring or Rubber Mount Isolators** to absorb residual vibration energy [8].

Figure 1. Springs or rubber isolators

b. Loose or Worn Mounting Hardware

The montage foundation upon which HVAC equipment rests is just as crucial as the equipment itself. Over time, bolts, nuts, and mounting brackets can loosen due to constant operation, thermal expansion/contraction, or improper installation [12]. When mounting hardware is compromised, vibrations are directly transmitted to the building structure, resulting *in the structural fatigue of the anchorage system of the duct system, and disturbing noises for building occupants* [33] and vibrations [32].

The technical solution: Must have a preventive maintenance program with regular torque checks and replacement of worn vibration mounts with Spring Isolators or Neoprene Pads [13].

Figure 2. Spring isolators or neoprene pads

c. Misaligned Components:

Misalignment between coupled components — typically between a motor and the driven equipment, the ventilation system — is a major source of vibration [14].

Causes include imprecise installation, thermal growth, or building settlement.

Misaligned shafts create excessive bearing loads, seal wear, and wasted energy.

The technical solution: Must use precision laser alignment tools during installation and re-check alignment periodically. Also, we must incorporate flexible connectors to accommodate minor residual misalignments [15].

Figure 3. Flexible connectors

d. Refrigerant Line Vibrations

Refrigerant line pulsations from compressors can cause excessive vibration if not properly supported [8].

Without proper restraint, vibration can lead to fatigue cracks and refrigerant leaks - costly and environmentally damaging.

The technical solution: Secure refrigerant lines with proper support at recommended intervals, avoiding rigid contact with the structure. Install Pipe Riser Anchors and Guides to dampen pulsations [16].

Figure 4. Pipe risers, anchors, and guides

e. Ductwork Vibration and Resonance

Improper duct sizing, high air velocities, or turbulent flow can excite duct wall vibrations.

When the air-flow-induced frequency matches the duct's natural frequency, resonance amplifies the vibration [17].

The technical solution: We must design the duct systems in accordance with ASHRAE guidelines to minimize turbulence and excessive velocities. It is obvious to install duct silencers or acoustic louvers to absorb noise and use Acoustic Barriers on duct exteriors to prevent resonance [18].

Figure 5. Duct silencers.

Figure 6. Acoustic louvers

The air flows that are used in HVAC installations [9] can be very varied depending on the operating hours of the installation, the indoor and outdoor air temperature, the temperature determined by the season in which the installation works, and the number of users.

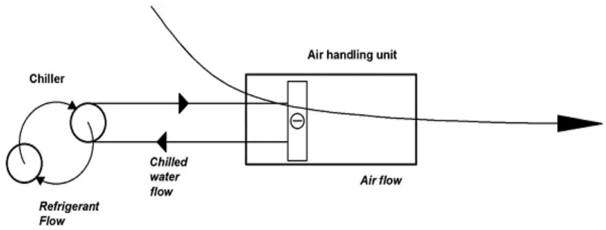

Figure 7. Different operating regimes of air in HVAC installations.

Thus, on long pipeline routes, air turbulence phenomena may appear that transform laminar flow regimes into turbulent flow regimes, which can be the generators of vibrations and noises, which may have the final effect of losing the tightness of the pipelines or even destroying the supports supporting the air ducts.

Modal analysis provides the user with a full arsenal of tools, beginning with data selection and parameter identification, to validation of results and modal shape animation.

The modal analysis of pipeline systems [10], [11] identifies the modes of self-vibration [19] and provides essential information for the configuration and distribution of supports to strengthen the structures and prevent future defects.

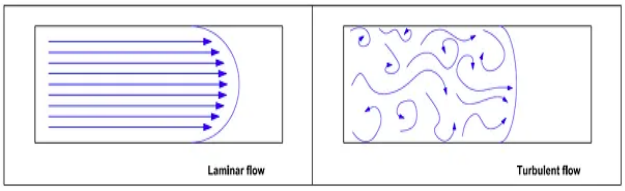

Figure 8. Different airflow regimes in HVAC installations.

For their configuration, it is also necessary to consider the influence of the turbulent air flow in the system.

3. MODAL ANALYSIS OF AN HVAC PIPE SYSTEM

So, the study based on modal analysis highlights the displacements on the three axes, the additional forces and moments induced by harmonic disturbing forces with constant amplitude.

The main objective is to analyze the dynamic behavior of the ventilation duct for a varied range of air flow rates and wall thicknesses of the circular duct.

We were focused on flow-induced vibrations and the possibility of resonance phenomena in certain sections of the ventilation system.

The modal analysis was carried out using the Bentley AutoPIPE CONNECT Advanced Edition [24] program, version 24.00.02.243, based on the demands presented above.

3.1. Technical data on ventilation ducting that are the subject of the modal analysis

The analyzed ventilation duct has a geometric configuration common in industrial applications and is schematically represented in Figure 9. It has the following main technical characteristics:

- Inner diameter of the ventilation ducts: 300 mm, constant parameter along the entire length.
- The elbows are oriented at a 90° angle and are arranged in areas where the flow direction changes.
- The rigid support that restricts movement in the vertical direction (Y-axis);
- The anchor-type supports are positioned at the ends, which block all six degrees of freedom (translations and rotations);
- The guide brackets are installed on the vertical sections to control the lateral displacements of the ducts.

The modal analysis was performed for three constructive variants of ducts, with different thicknesses, that are made of the same metal material, ASTM A53 Grade A carbon steel, which has a yield strength of 205 MPa.

We analyzed three cases of thicknesses of the pipe walls of 0.2 mm, 0.4 mm, and 0.6 mm, with the scope to evaluate the influence of the rigidity of the duct on vibrational behavior.

Based on the simulations carried out, five vibration modes were identified, representative of the analyzed configuration.

The air duct system conveys air for a range of volume flows ranging from 1000 m³/h to 7000 m³/h, with a temperature of 20°C and with a pressure of 0.02 kgf/cm² (equivalent to 1.96 kPa).

The six tables correspond with the three types of thickness of the air pipe, show the maximum excitation frequency that has the greatest influence of the average mass of the pipe, which results in a mass, this force that appears on the Z axis, and reprezent the disturbing factor, which leads to the deformation of the supports supporting the pipe as well as to the deformation of the connection elements between the straight sections and the bends that are part of the air transport system being studied.

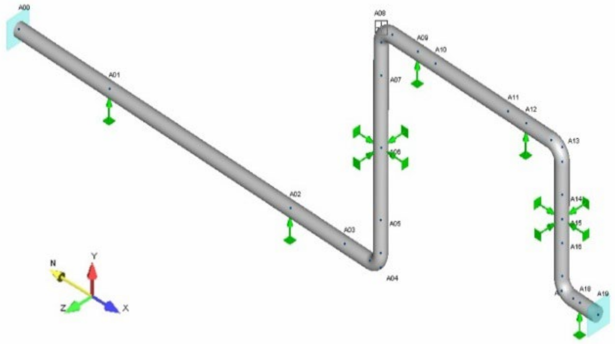

Figure 9. Geometric configuration of the air transport duct system.

3.2. The case study 1

The first case study is based on the system of circular air transport ducts with a length of 30 m and a specific thickness of 2 mm, with a total weight of 34,7 kg, as presented in Figure 9.

Table 1A. The vibration modes with specific participations corresponding to the modal masses on the X, Y, and Z axes for circular ducts with a thickness of **0.2 mm**.

Mode no.	Frec. [Hz]	Period [s]	Modal mass X axis [%]	Modal mass Y axis [%]	Modal mass Z axis [%]
1	2.5214	0.397	0	0	0.99
2	**14.295**	**0.07**	**0**	**0**	**57.911**
3	17.164	0.058	21.327	0.124	0
4	21.747	0046	-0	0	0.03
5	24.366	0.041	1.102	26.895	0

Table 1B. The vibration modes with the average modal mass cumulate drive on axes X, Y, and Z, for the air circular ducts, with a thickness of **0.2 mm**.

Mode no.	Frecv. [Hz]	Period [s]	Cumulative average mass [%]	The weight influence depends on the average mass [kg]
1	2.5214	0.397	0.33	0.114
2	**14.295**	**0.07**	**19,304**	**6,698**
3	17.164	0.058	7,15	2,481
4	21.747	0046	0.01	0,003
5	24.366	0.041	9.332	3.238

Thus, modes 2, 3, and 5 show high participation factors and entrained modal masses, indicating an important contribution to the overall dynamic response of the pipe for all wall thickness variants analyzed (see Table 1A).

From Table 1B, it is obvious that mode 2, which corresponds to an excitation frequency of 14.295 Hz, drives on the Z-axis the largest modal mass (average), which causes the appearance of a (strong) force-weight on the Z-axis in the amount of 6.698 kg, which leads to the appearance of important deformations (defects) in the Z-axis area.

3.3. The case study 2

The second case study is based on a circular air transport duct with a length of 30 m and a thickness of 4 mm, with a total weight of 69,74 kg, as presented in Figure 9.

Table 2A. The vibration modes with the specific participations that correspond to the modal masses on the axes X, Y, and Z, for circular ducts, with thickness **0.4 mm**

Mode no.	Frec. [Hz]	Period [s]	Modal mass X axis [%]	Modal mass Y axis [%]	Modal mass Z axis [%]
1	2.7886	0.359	0	0	1.038
2	**15.0491**	**0.066**	**0**	**0**	**58.19**
3	19.3585	0.052	22.851	0.09	0
4	23.2704	0.043	0	0	0.445
5	26.7269	0.037	0.852	27.173	0

Thus, modes 2, 3, and 5 show high participation factors and entrained modal masses, indicating an important contribution to the overall dynamic response of the pipe for all wall thickness variants analyzed (see Table 2A).

It is obvious from the Table 2B that mode 2, which corresponds to an excitation frequency of 15.0491 Hz, drives the largest modal mass (average) on the Z axis, which causes the appearance of a (strong) force-weight on the Z axis in the amount of 13.458 kg, which can lead to the appearance of important deformations (defects) in the Z axis area.

Table 2B. The vibration modes with the average modal mass cumulate drive on axes X, Y, and Z, for circular ducts, with a thickness of **0.4 mm**

Mode no.	Frec. [Hz]	Period [s]	Cumulative average mass [%]	The weight influence depends on the average mass [kg]
1	2.7886	0.359	0.342	0,237
2	**15.0491**	**0.066**	**19.393**	**13,458**
3	19.3585	0.052	7.644	5,304
4	23.2704	0.043	0.145	0,100
5	26.7269	0.037	9.342	6,483

3.4. The case study 3

The third study is based on the system of circular air transport ducts with a length of 30 m and a specific thickness of 6 mm, with a total weight of 104,2 kg, as presented in Figure 9.

Table 3A. The vibration modes with the specific participations that correspond with the modal masses on the axes X, Y, and Z, for circular ducts, with a thickness of **0.6 mm**.

Mode no.	Frec. [Hz]	Period [s]	Modal mass X axis [%]	Modal mass Y axis [%]	Modal mass Z axis [%]
1	3.0487	0.328	0	0	1.082
2	**15.469**	**0.065**	**0**	**0**	**57.682**
3	21.0183	0.048	23.917	0.095	0
4	24.3513	0.041	0	0	1.264
5	28.608	0.035	0.738	27.252	0

Table 3B. The vibration modes with the average modal mass cumulate drive on axes X, Y, and Z, for circular ducts, with a thickness of **0.6 mm**:

Mode no.	Frec. [Hz]	Period [s]	Cumulative average mass [%]	The weight influence depends on the average mass [kg]
1	3.0487	0.328	0.362	0,370
2	**15.469**	**0.065**	**19.223**	**19,684**
3	21.0183	0.048	8.004	8,196
4	24.3513	0.041	0.425	0,435
5	28.608	0.035	9.33	9,553

Thus, modes 2, 3, and 5 show high participation factors and entrained modal masses, indicating an important contribution to the overall dynamic response of the pipe for all wall thickness variants analyzed (see Table 3A).

From Table 3B, it is evident that mode 2, which corresponds to an excitation frequency of 15.469 Hz, drives the largest modal mass (average) on the Z axis, which causes the appearance of a (strong) weight on the Z axis in the amount of 19.684 kg, which can lead to the appearance of significant deformation (defects) in the Z axis area.

3.5. Results and discussions

Based on the modal analysis results, the dominant vibration modes of the piping system are those in which a significant percentage of the assembly's total mass is entrained.

Based on the largest cumulative masses (%) respectively based on the weights obtained depending on the 3 sheet thicknesses (2 mm, 4 mm and 6 mm), values that were obtained only on the Z axis for close frequencies, included in the frequency range from 14.295Hz to 15.469 HZ we centralized specific results in Table 4, represented graphically in the diagram in Figure 10.

Table 4. The corresponding mass results depend on wall thickness and frequency

Wall thickness [mm]	Frec. [Hz]	Period [s]	Cumulative average mass [%]	The weight influence depends on the average mass [kg]
2	14,29	0,07	19,304	6,698
4	15,04	0,066	19,393	13,458
6	15,46	0,065	19,223	19,684

We observe in Table 4 that the parameters of frequency (Hz), period (s), and cumulative total mass, which had the largest participation on the Z axis, have values that remain constant with small variations.

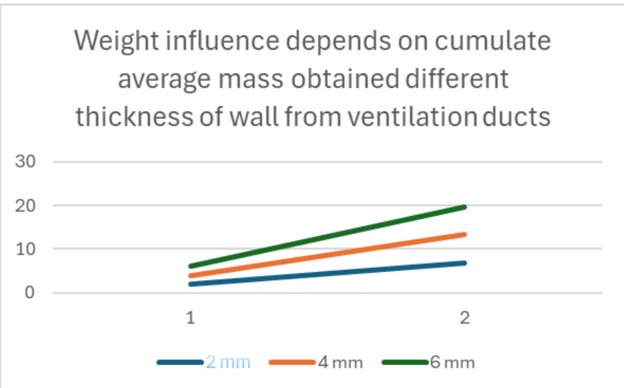

Figure 10. Graphic representation of cumulating average mass influences depending on the duct's wall thickness, which may be 2 mm, 4 mm, or 6 mm.

The conclusion that emerges is that average cumulative masses (%) can be obtained, respectively, the weights that influence the pipe and its support structure for much smaller values of the pipe wall thickness, that is, for approximately the same frequency and period values, on the Z axis, which will allow the installation of a much lighter support structure [20].

4. AIR TURBULENCE MODELING

4.1 Determination and analysis of the characteristic parameters of air flow

The piping system that includes the segment of ventilation ducts that was studied before conveys air at a temperature of 20°C, for a range of volume flows ranging from 1000 m³/h to 7000 m³/h (1000, 2000, 3000, 4000, 5000, 6000, and 7000 m³/h).

To characterize the flow regime, the Reynolds number [21] is determined for each analyzed flow, an essential parameter for classifying the flow type (laminar, transitional, or turbulent).

$$Re = \frac{\rho \cdot u \cdot L}{\mu} \tag{1}$$

where:

- Re is the Reynolds number that characterizes the air flow regime.
- ρ is air density at 20 gr. C $= 1.2041\,\frac{\mathrm{kg}}{\mathrm{m}^3}$;
- u is the flow rate of the fluid, which is determined from the relationship between the flow rate and the diameter of the pipe.
- L is the inner diameter of the pipe, 300 mm.
- μ is the dynamic viscosity of the air at 20 °C, μ = 0,0000182 Pa * s.

A study is carried out on the first elbow at 90°, calculating the Reynolds number for seven different air flows, beginning with 1000 m^3/h until 7000 m^3/h flow that are characterized by specific fluid flow speeds through a circular air transport duct with a diameter of 300 mm (0.3 m), dates that are presented in Table 5.

Table 5. The specific Reynolds numbers and air flow speed for the seven different air flow regimes

No. item.	Air flow [m^3/h]	Air speed [m/s]	Reynolds number
1.	1000	0,93	78036
2.	2000	1,85	156073
3.	3000	2,78	234109
4.	4000	3,70	312146
5.	5000	4,63	390182
6.	6000	5,56	468219
7.	7000	6,48	546255

The Reynolds number was calculated to be between 18378 and 128643, which corresponds to the turbulent flow region on Moody's diagram in Figure 11 [22].

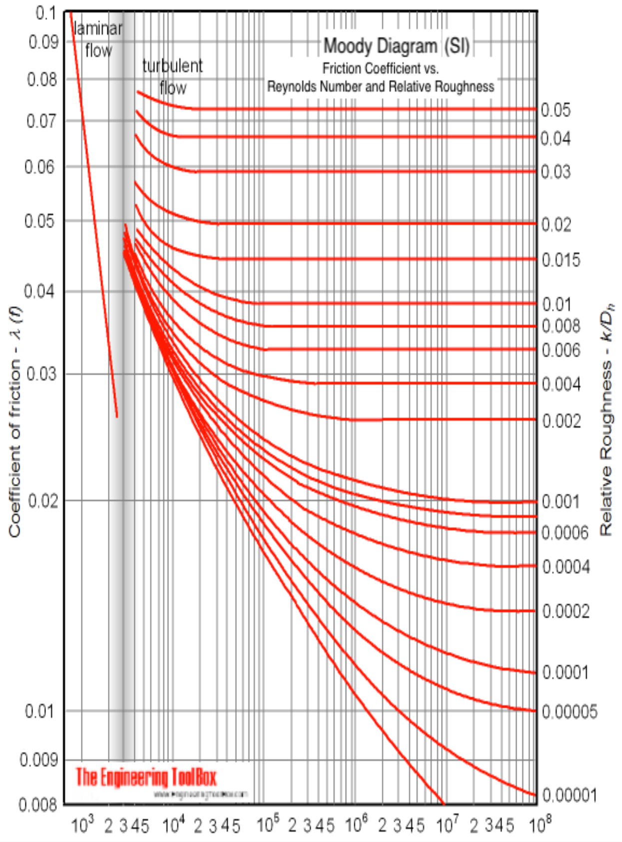

Figure 11. Moody's diagram [22]

4.2. The determination of the Strouhal number and the excitation frequency

To determine the Strouhal number as a function of the Reynolds number, the special diagram in Figure 12 is used. The relationship between the Strouhal and Reynolds numbers was used.

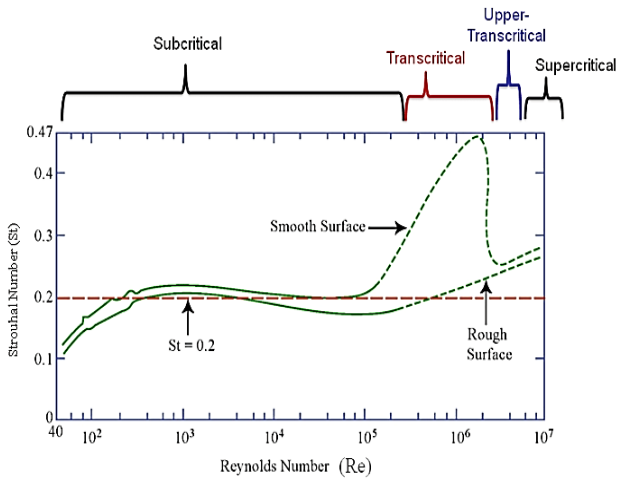

Figure 12. The graphic correspondence between Reynolds number and Strouhal number [23, 33]

Using that diagram to determine the Strouhal number [23, 33] in correspondence with the Reynolds number, were adopted for the elbow 90° the Strouhal number values of 0.2, corresponding to the Reynolds number of 73510, and 0.3, corresponding to the other Reynolds number values.

For each case analyzed of the 90° elbow, the flow excitation frequency was determined by applying the relation:

$$f = \frac{S_t \cdot U}{D} \tag{2}$$

where:

- f is the excitation frequency
- S_t is Strouhal's number
- U is the fluid flow rate from the relationship between flow rate and pipe diameter
- D is the inner diameter of the pipe on various sections of bends, tees, and valves.

Table 6. The results correspond to Reynolds numbers, Strouhal numbers, and air flow speeds and excitation frequency for the seven-flow air regime

Air flow [m³/h]	Air speed [m/s]	Reynolds number	Strouhal number [%]	Excitation frequency [Hz]
1000	3,93	78036	0,2	2,6212
2000	7,86	156073	0,2	7,8635
3000	11,80	234109	0,3	11,7952
4000	15,73	312146	0,3	15,7270
5000	19,66	390182	0,3	19,6587
6000	23,56	468219	0,3	23,5905
7000	27,52	546255	0,3	27,5222

4.3. Results and discussions

Based on Table 6, when we obtain the specific value for air flow that is in correspondence with air speed and the excitation frequency value, which are the bases of the graphic representation from Figure 13.

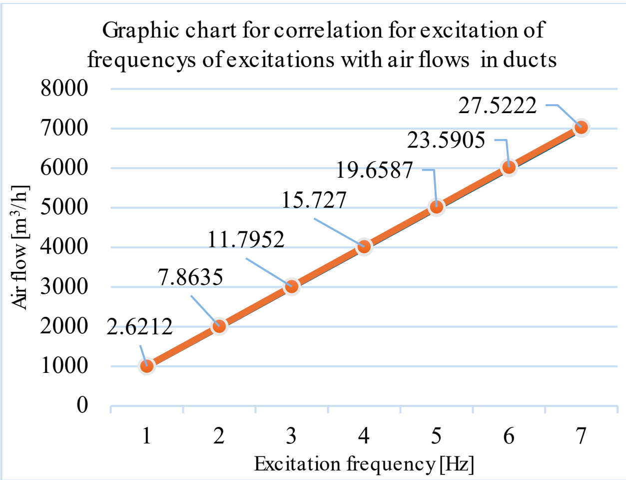

Figure 13. A graphic chart for correlation for the excitation of frequency of excitations with air flows in air ducts

5. CONCLUSIONS

The modal synthesis completed with the dynamic analysis that was performed on the transport air system revealed that, in the case of 90° bends, the excitation frequencies determined by the Vortex Shedding [28] type mechanism coincide or are close to the natural vibration frequencies obtained by the modal analysis performed in the Bentley AutoPIPE program [24].

In all these cases, vibration modes 2, 3, and 5 fell within the range of frequencies generated by vortex shedding, indicating the possibility of the occurrence of the local resonance phenomenon in these regions.

Based on modal analysis for three constructive variants of the ducts, corresponding to sheet thicknesses of 0.2 mm, 0.4 mm, and 0.6 mm, we obtained the value of dangerous frequency around 15 Hz.

It is obvious that the flow rate analysis shows that the flow rate of 4000 m3/h, the ventilation elbows represent vibrationally critical areas, susceptible to amplified hydrodynamic vibrations [29], [30].

It is found that the harmonic disturbing force with constant amplitude that simulates the turbulent flow of the fluid in normal operation mode induces displacements, forces, and significant moments additional to those given by the weight of the pipe system, temperature, and working pressure [25], [32]. These vibration modes can be considered critical regarding dynamic behavior, as they describe eigen shapes associated with significant deformations and local resonance potential in the presence of external excitations with close frequencies.

The induction of additional forces on the elastic supports will require their adjustment or even changing these elastic supports [26].

The applications and future scope of the study, using the simulation Bentley AutoPIPE CONNECT Advanced Edition software to obtain, based on simulation method used, real function parameters, the dangerous values of the modal proper frequencies of air ducts that may be combined with the calcul of excitation frequencies obtained from the air flow to avoid the future damages of the system transport ducts of air.

REFERENCES

[1] Kazimierz Peszyński, Lukasz Olszewski, Emil Smyk, and Daniel Perczyński, Analysis of the velocity distribution in different types of ventilation system ducts, *EPJ Web of Conferences,* 180, 02081 (2018) EFM 2017. https://doi.org/10.1051/epjconf/201818002081

[2] Importance of Resonance Detection and Avoidance in HVAC Systems, *DATA CENTER FRONTIER*, https://www.datacenterfrontier.com/sponsored/article/55245955/importance-of-resonance-detection-and-avoidance-in-hvac-systems

[3] M. Siba, W. Wanmahmood, M. Zaki Nuawi, R. Rasani, M. Nassir, Flow-induced vibration in pipes: challenges and solutions - a review Journal of Engineering Science and Technology, Vol. 11, No. 3 (2016), © School of Engineering, Taylor's University pp. 362-382.

[4] The Isolator Newsletter – August 2025 – Vol 78 – https://kineticsgroup.ae/5-critical-vibration-issues-killing-your-hvac-equipment-and-how-to-fix-them/

[5] ISO 10816-3, 2022 Mechanical vibration — Measurement and evaluation of machine vibration Part 3: Industrial machinery with a power rating above 15 kW and operating speeds between 120 r/min and 30 000 r/min. https://www.iso.org/standard/78311.html

[6] ICONAMMA2018, IOP Publishing, *IOP Conf. Series: Materials Sciences and Engineering*, 577 (2019), 012140, https://doi:10.1088/1757-899X/577/1/012140

[7] *Pumping Station Design* (Third Edition), 2008, Pages 22.1-22.65, chapter 3 – pp 3.1-3.37, chapter 4, pp. 4.1-4.41, 6, 7, 10, 11, 12, 14, 15, 22.

[8] ASHRAE Handbook – *HVAC Systems and Equipment*, 2020. https://www.ashrae.org/about/news/2020/2020-ashrae-handbook-focuses-on-systems-and-equipment

[9] *Flow in HVAC systems explained* – by Albrand Veldhuizen, 30/03/2021. https://www.heinenhopman.com/20210330-flow-in-hvac-systems-explained/

[10] What Is Modal Analysis and Why Is It Necessary? Caesar II Piping Modal Analysis Steps, Anup Kumar Dey, https://whatispiping.com/modal-analysis/

[11] PIPING WORLD – The piping Engineering Resource, https://www.piping-world.com/modal-analysis

[12] ASHRAE Handbook – HVAC Applications, 2023. https://www.ashrae.org/technical-resources/ashrae-handbook/2023-ashrae-handbook-hvac-applications

[13] *McGraw-Hill HVAC, Engineer's Handbook,* 2013, chromeextension://efaidnbmnnnibpcajpcglclefindmkaj/https://www.arma.org.au/wpcontent/uploads/2017/03/HANDBOOK-OF-AIR-CONDITIONING-AND REFRIGERATION-Second-Edition-McGraw-Hill.pdf

[14] *ASHRAE Research Project RP-755*, 1997. https://www.osti.gov/biblio/653238

[15] *ASHRAE Handbook – Fundamentals*, 2021. https://www.ashrae.org/technical-resources/ashrae-handbook/description-2021-ashrae-handbook-fundamentals.

[16] Bies & Hansen, 2017. https://www.taylorfrancis.com/books/mono/10.1201/9781351228152/engineering-noise-control-david-bies-colin-hansen-carl-howard.

[17] SMACNA HVAC Systems Design, 2006. chrome-extension://efaidnbmnnnibpcajpcglclefindmkaj/https://kh.aquaenergyexpo.com/wp-content/uploads/2023/01/HVAC-Duct-Construction-Standards.pdf.

[18] ASHRAE Handbook – Fundamentals, 2021. https://www.ashrae.org/technical-resources/ashrae-handbook/description-2021-ashrae-handbook-fundamentals.

[19] Manuel Bautista Ordoñez, Maria Alzira de Araújo Nunes, Duct system modeling through the Jose HVAC component mode synthesis for structural vibration analysis, *24th ABCM International Congress of Mechanical Engineering,* December 3-8, 2017, Curitiba, PR, Brazil. https://www.researchgate.net/publication/323204553_HVAC_duct_system_modeling_through_the_component_mode_synthesis_for_structural_vibration_analysis

[20] Pattaramon Tanadecha, Kunthakorn Khaothong, Analysis of the alternative air ductwork by Numerical airflow behavior combined with the New Economic index and standard, https://doi.org/10.1016/j.enbenv.2024.04.004
[21] Basic Flow Measurement Laws, https://www.sciencedirect.com/topics/engineering/reynolds-number
[22] Calculate fluid flow friction coefficients from a Moody diagram, https://www.engineeringtoolbox.com/moody-diagram-d_618.html
[23] Diagram for relationship of Strouhal number to Reynolds number, https://www.researchgate.net/figure/Relation-of-trouhal-Number-and-Reynolds Number_fig1_265496181
[24] Bentley, *AutoPIPE CONNECT*, Advanced Edition, https://www.bentley.com/software/autopipe/
[25] N. Posea, A. Anghel, N. Grigore, V. Mincu, *Statics and Dynamics Piping Systems*, Bucharest, Romanian Academy Publishing House, 1996.
[26] P. Bratu, *Analysis of Elastic Structures*, Bucharest, Impuls Publishing House, 2011.
[27] S. ZIADA and S. SHINE, Strouhal numbers of flow-excited acoustic resonance of closed side branches, *Journal of Fluids and Structures*, vol. 13, no. 1, pp. 127–142, Jan. 1999, https://www.sciencedirect.com/science/article/abs/pii/S088997469890189X?via%3Dihub; https://doi.org/10.1006/jfls.1998.0189
[28] Z. Chen, Vortex Shedding in a Tee with a Closed Branch, *Becht*, Mar. 04, 2024. Available online: https://becht.com/becht-blog/entry/vortex-shedding-in-a-tee-with-a-closed-branch/
[29] Eduard Naudascher, *Flow-induced Vibrations: an Engineering Guide*, Routledge, 2017.
[30] Y. IWAMOTO, M. KONDO, H. MINAMIURA, M. TANAKA, and H. YAMANO, Unsteady Flow Characteristics in a 90 Degree Elbow Affected by Developed, Undeveloped and Swirling Inflow Conditions, *Journal of Fluid Science and Technology*, vol. 7, no. 3, pp. 315–328, 2012, https://doi.org/10.1299/jfst.7.315
[31] P. Bratu, *Dynamic isolation*, Bucharest, Impuls Publishing House, 2021.
[32] G. Nicolae, M. C. Nitu, P. Bratu, M. Iliescu, E. Furdui-Lungut, and M. Dogaru (2025), Vibrations Transmitted to The Human Body Under the Dynamic Action of Surfaces and Mechanical Contact Points with Impact on Human Health, *Romanian Journal of Acoustics and Vibration*, 22(1), 66-72.
[33] M.C. Nițu; M. Iliescu, E. Furdui-Lunguț, Specific Protection Requirements and Psychosensory Effects To the Noise Generated by Construction Equipment, *ACTA TECHNICA NAPOCENSIS - Series: APPLIED MATHEMATICS, MECHANICS, and ENGINEERING*, [S.l.], v. 68, n. 1 & 2, jun. 2025, ISSN 2393–2988.